

ARTICLES

Range of spectral correlations in pseudointegrable systems: Gaussian-orthogonal-ensemble statistics in a rectangular membrane with a point scatterer

Richard L. Weaver¹ and Didier Sornette²

¹*Department of Theoretical and Applied Mechanics, University of Illinois, 104 South Wright Street, Urbana, Illinois 61801*

²*Laboratoire de Physique de la Matière Condensée, CNRS URA 190, Université de Nice–Sophia Antipolis, Faculté des Sciences, 06108 Nice Cedex 2, France*

(Received 6 April 1995)

Conventional wisdom holds that a finite reverberant system with chaotic ray trajectories will have, at high frequencies, eigenvalue statistics identical to those of the Gaussian orthogonal ensemble (GOE) of random matrices. It also holds that a nonchaotic system will have simple Poissonian statistics. Recent experiments on the eigenvalues of elastic blocks with angled cuts and recent calculations of the eigenfrequencies of membranes with staircaselike jagged boundaries and the eigenfrequencies of a rectangular domain with a single isotropic point scatterer have, however, found GOE statistics even in these pseudointegrable systems—even though all rays in such systems are nonchaotic. In this work, the rectangular domain with a single isotropic point scatterer is studied further. In contrast to recent related work, the scatterer is characterized here by its t matrix and scattering cross section. It is shown that the long-range level repulsion in this system is not in precise accord with the predictions of the GOE, nor is the long-range spectral rigidity. GOE does, though, correctly describe the short-range statistics. A quantitative prediction for the range in which GOE applies is advanced based upon the lifetime of a ray against mixing—i.e., based upon the scattering cross section of the scatterer. This prediction is corroborated by numerical calculations of the eigenfrequencies.

PACS number(s): 05.45.+b, 03.65.-w, 03.40.Kf, 43.40.+s

I. INTRODUCTION

There is substantial modern literature existent on a subject loosely termed “quantum chaos” [1–3], regarding issues related to the correspondence between classical mechanics of particles with ergodic dynamics and quantum mechanics in the limit of a small Planck constant. That this correspondence, which is much like the high-frequency correspondence between ray acoustics and eigenmode acoustics, is unclear has long been appreciated (see, for example, Gutzwiller’s discussion in [1]). There is nevertheless a general consensus that a finite time reversal invariant system with chaotic ray trajectories will have, at high frequencies, eigenvalue statistics identical to those of the Gaussian orthogonal ensemble (GOE) of random matrices [4,5] and that these statistics are the sign in the quantum spectrum of the underlying chaotic classical mechanics. It is furthermore believed that systems whose classical ray mechanics is nonchaotic will have high-frequency spectra with simple Poissonian statistics.

The first of these beliefs is well supported by an impressive array of numerical experiments [6–8] evaluating the eigenspectra of so-called “billiard problems.” Billiards have classical ray trajectories that reflect specularly from the walls. The associated eigenproblem concerns the eigenfrequencies of the billiard shape with reflecting boundary conditions, e.g., Dirichlet. As for most shapes

presenting focusing or defocusing boundaries, the Sinai billiard and the Bunimovich stadium have ray trajectories that are almost all chaotic. The spectral statistics of these systems have been found to correspond, with a high degree of confidence, to those of the spectrum of the GOE [4,5]. There are also laboratory confirmations of the correspondence, carried out on the vibrational eigenfrequencies of stadium-shaped plates and the microwave eigenfrequencies of stadium-shaped cavities [9].

The second of the beliefs is, however, much less well supported. The belief has been clearly stated: “When the geometrical acoustics limit does not correspond to a chaotic motion, but rather to a regular one with nearby trajectories diverging at most as a power law of time, one expects that the corresponding spectrum is not predicted by the GOE but is rather Poissonian” [10]. That rectangular, circular, and elliptical [8,11] billiards have Poissonian statistics is well appreciated. There are, however, certain classical ray systems that, while nonintegrable, nevertheless have regular nonchaotic ray dynamics. Numerical [12–15] and laboratory evidence [16], however, suggests that these systems have eigenstatistics like those of the GOE. How then are we to understand the nature of the correspondence? What aspects of the classical dynamics lead to GOE statistics? In the next section we briefly review the evidence for GOE-like statistics in these regular systems and advance, on physical grounds,

a hypothesis that accounts for the statistics of these systems. The hypothesis predicts the range over which GOE statistics should and should not apply. The subsequent sections examine the simple and numerically tractable case of a point scatterer in a rectangular membrane and show that its statistics, when analyzed more closely, are not precisely those of the GOE, but do conform to the predictions of the hypothesis.

II. EVIDENCE FOR GOE-LIKE STATISTICS IN CLASSICALLY REGULAR SYSTEMS

Our interest in this question began some years ago when one of us [16] showed that the statistics of the measured elastodynamic eigenfrequencies of aluminum blocks corresponded to those of the GOE. The nominally rectangular blocks used in that study had slits cut in them to eliminate the reflection symmetries, but they had no explicit focusing or defocusing boundaries. Thus ray trajectories in these blocks were nonchaotic. From the point of view of the second belief above, the appearance of the GOE statistics was therefore puzzling [10]. This belief in the correspondence of regular ray trajectories with Poissonian statistics is mostly based upon experience with the scalar wave equation. It might be that vector elastodynamic systems such as those of the blocks are sufficiently different from the scalar systems that they do not conform to the conventional understanding. That possibility was discussed and discounted in Ref. [10]. Instead it was suggested there that what is relevant is the amount of chaos present in the classical motion at the scale of the wavelength. It was further asserted that for much higher frequencies such that wavelengths are of the order of the slit width one must recover regular ray trajectories and Poissonian statistics.

Similar behavior was observed in a numerical study [14] of a rectangular billiard, of size L , with a large number of small rectangular pieces, of size l , removed from the edges. As the size of the pieces $l \rightarrow 0$ the number of pieces went to infinity in such a way that the system resembled, in that limit, a smooth bounded Sinai billiard. At nonzero l the classical ray trajectories are regular and conventional wisdom would predict Poissonian eigenstatistics. Nevertheless, the numerically determined eigenfrequencies of the membrane were found to obey GOE statistics as long as the wavelength was greater than l . As hypothesized there, and in Ref. [9] in regard to the elastodynamic system, the wave is presumably not sensitive to the exact shape of the billiard, but rather to its shape on a spatial scale with limited resolution comparable to a wavelength.

In a pair of papers Seba [12] and Albeverio and Seba [13] argue against this hypothesis. They discuss the statistics of the eigenfrequencies of a rectangular membrane with an isotropic point scatterer, usually placed at the exact center. Almost all ray trajectories in this system are nonchaotic; only the rare ray that exactly strikes the scatterer will be aware that the system is other than a simple rectangle. It was nevertheless proved that the level spacing distribution exhibits level repulsion. Seba's numerically determined level spacing distribution appeared

to agree with the predictions of the GOE. In Seba's system there is no length scale to which the wavelength may be compared. There is thus no possibility of recovering Poissonian statistics at high frequencies; the above hypothesis cannot explain Seba's results. Later Shigehara [15] confirmed Seba's conclusions and demonstrated that Poisson-like statistics are regained if the scatterer is in some sense weak.

It is conjectured here that the GOE character of the statistics observed in the aluminum blocks [16] and in the staircase edged membranes [14] is related to the GOE character observed by Seba and is not due to a finite ratio of wavelength to some other relevant length scale, such as stair size or slit width. It would instead be due to scattering or diffraction at the pointlike edges and corners, analogous to the isotropic point scattering in the systems studied by Seba and co-workers [12,13] and Shigehara [15]. One consequence of this conjecture is that the statistics in the aluminum block and in the staircase edged membrane would retain apparent GOE statistics even in the high-frequency limit, regardless of the ratio of wavelength to any structural length scales.

Modal repulsion, and, in general, spectral correlations, between different modes is understood to occur when the modes or the associated ray trajectories in some sense occupy the same region in phase space. For this reason classically chaotic systems, any ray of which occupies all of the phase space, are understood to have fully developed GOE eigenstatistics. Such arguments, however, cannot be quite correct. Different modes have different eigenfrequencies; they thus occupy different energy shells in phase space. They *do not* occupy the same volumes in phase space. This counterargument has a significant flaw whose analysis, we believe, sheds light on the GOE character of the eigenstatistics in the systems discussed above. The flaw lies in the supposition that the energy, or frequency, can be specified with arbitrary precision. The uncertainty principle tells us, however, that the frequency must be imprecise to within an amount $\Delta\omega$ after a time $T = 2\pi/\Delta\omega$.

Thus it is also important to ask how rapidly phase space is filled. One imagines that ray trajectories spread over an energy shell in phase space while the thickness of that shell simultaneously shrinks. In a classically chaotic system the rays fill the shell rapidly, long before significant thickness reduction has taken place; thus the phase volumes of neighboring modes overlap significantly and spectral correlations result. Two modes, separated by a frequency difference $\Delta\omega$, are therefore correlated only if they explore the same region of phase space and do so within the allotted time. This is the reason that unstable orbits can scar the eigenstates of classically chaotic systems. The orbits may be unstable, but their Lyapunov exponents are weak in some sense compared to the modal spacings [17]. In his discussion of scarring, Heller [6] has emphasized the importance of a quantity he calls the break time, defined as the time necessary to resolve two modes separated by an average level spacing $\tau = 2\pi\rho$, where ρ is the level density: "While a ray system has an infinite amount of time to develop, the corresponding wave system is given only a finite time; thus eigenstates

can be expected to be less globally distributed than the infinite time average of a classical trajectory" [6]. It may be noted that Shudo and Shimizu [18] also discussed the rate at which a single ray trajectory fills phase space in their rhombus-shaped billiard.

From this perspective we see that classical chaos is not the *sine qua non* for spectral correlations. Indeed, we see that spectra correlations over a range $\Delta\omega$ should be expected whenever ray trajectories fill their phase space shells within a time $2\pi/\Delta\omega$. This may occur even in systems with regular trajectories. The weak level density fluctuations associated with periodic orbits of chaotic systems is a special case of the hypothesized limit of applicability of the GOE. The nonuniversal behavior of the eigenstatistics over these ranges is related to the finite time for the rays, even in a chaotic system, to ergodically fill phase space shells.

We thus suppose that eigenstatistics in systems such as that discussed by Seba and co-workers [12,13], Shigehara [15], Cheon and Cohen [14], Weaver [16], and Shudo and Shimizu [18] are correlated over ranges $\Delta\omega=1/T$, where T is the time for a typical packet of energy to spread over phase space. This happens only after it scatters from Seba's point scatterer or diffracts from a sharp corner. We furthermore suppose that the eigenstatistics are uncorrelated over longer ranges. If σ represents the total scattering cross section in the system of area A , a typical ray will scatter after a time of the order of $A/(\sigma c)$ equal to, if the rays mix well in real space, the mean free ray time in a two-dimensional geometry. Thus one expects correlations over ranges $\Delta\omega$ less than or equal to $(\sigma c)/A$. But $\delta\omega$, the mean level spacing, is $c\lambda/A$. Expressed non-dimensionally therefore, the correlation range will be σ/λ . In Seba's system one can assign a scattering cross section σ to the point scatterer that is of the order of the wavelength λ . This is the quantitative formulation of our proposal that, however small the wavelength is, the scattering cross section due to diffraction shrinks to zero with the wavelength at the same rate when one goes to the geometrical regime. As a consequence, the effect of the scatterer remains of the same relative strength at all frequencies, in agreement with our hypothesis. Thus one expects correlation ranges in his systems to extend only over about one mean level spacing. Seba did not publish data on long range correlations, but one can argue (see below) that his system must have very little spectra rigidity. One can also barely detect a failure of GOE predictions at longer ranges in his plots of the nearest-neighbor level spacing distribution. Shigehara [15] did publish data on long-range spectral rigidity that did show the failure of GOE statistics at these ranges. Similarly Shudo and Shimizu [18] showed, in their study of a rhombus billiard, that the failure of GOE statistics is confined to the longer ranges. This is precisely what the present hypothesis predicts: GOE statistics are failing over non-dimensional ranges of the order or greater than σ/λ .

The remainder of this paper is devoted to a further study of the system introduced by Seba consisting of a point scatterer in a rectangular domain. We particularly wish to confirm whether, as is predicted by the present hypothesis, the apparent GOE statistics fail at longer

ranges. Section III derives an analytic expression whose roots determine the eigenfrequencies of the system and is readily evaluated numerically. The statistics of those eigenfrequencies are presented in Sec. V.

Shigehara [15] has recently studied a similar system, with an emphasis on a mathematical calculation of the strength of the scatterer (which poses problems in two dimensions [18]). In that work, the physical meaning of the strength of the scatterer remained elusive and there was no connection drawn between the scatterer strength and the scattering cross section. In the present paper the physical meaning of the scatterer strength follows straightforwardly from a formulation in terms of the familiar and natural t matrix; a consequent interpretation in terms of a cross section is then simple. This formulation also obviates the diverging sums and associated ultraviolet cutoffs that obscured Shigehara's main points. The consequent simplicity also allows what we think is a better control of the precision of the calculations. Finally, as above, the connection with scattering cross section allows us to propose a clear physical criterion for the appearance of spectral rigidity in terms of the time needed for a wave packet to explore its phase space. An important prediction is that the range of spectral rigidity should increase with the number of scatterers. Interestingly, Shigehara reports preliminary results that indicate that the GOE correspondence increases with the number of scatterers.

III. ANALYSIS OF THE RECTANGULAR DOMAIN WITH POINT SCATTERER

The eigenvalue problem for the reduced wave equation in a reverberant system with a point scatterer is readily formulated in terms of the eigenfunctions of the same domain without the scatterer and in terms of the operator that describes the point scatterer in an unbounded domain. One advantage of such a formulation is that it is straightforward and familiar and its physical meaning is unambiguous and natural. In this section we present that procedure.

The bare rectangular domain $0 < x < L_x$, $0 < y < L_y$ with Dirichlet boundary conditions and unit wave speed has a Green's function that satisfies the inhomogeneous Helmholtz equation

$$[\omega^2 + \nabla^2]G_0(\mathbf{r}, \mathbf{r}'; \omega) = \delta^2(\mathbf{r} - \mathbf{r}') ,$$

$$G_0(\mathbf{r} \in \text{boundary}, \mathbf{r}'; \omega) = 0 . \quad (1)$$

The normal modes $\phi_{nm}(x, y) = \phi_{nm}(\mathbf{r})$ of the homogeneous equation

$$\nabla^2 \phi_{nm}(\mathbf{r}) = -\omega_{nm}^2 \phi_{nm}(\mathbf{r}), \quad \phi(\mathbf{r} \in \text{boundary}) = 0$$

are

$$\phi_{nm} = (4/L_x L_y)^{1/2} \sin(n\pi x/L_x) \sin(m\pi y/L_y) ,$$

$$\omega_{nm} = (n^2 \pi^2 / L_x^2 + m^2 \pi^2 / L_y^2)^{1/2} . \quad (2)$$

The Green's function may be written in terms of the normal modes

$$G_0(\mathbf{r}, \mathbf{r}'; \omega + i\epsilon) = \sum_{n,m} \phi_{nm}(\mathbf{r}) \phi_{nm}(\mathbf{r}') / [(\omega + i\epsilon)^2 - \omega_{nm}^2], \quad (3)$$

where the sum is over all positive n and m and where it has been realized that G is well defined only if ω is in the upper half complex plane. In the remainder of this paper ϵ will be understood to be infinitesimal and positive.

The Green's function for an unbounded domain is the outgoing Hankel function

$$G^\infty(\mathbf{r}, \mathbf{r}'; \omega) = -(i/4)H_0^{(1)}(|\mathbf{R}| \omega), \quad (4)$$

where \mathbf{R} is the vector connecting source and receiver $\mathbf{R} = \mathbf{r} - \mathbf{r}'$. A point scatterer in any dimension equal to or greater than 2 cannot be represented in terms of a scattering potential [19]. Therefore Seba defined his point scatterer [12] by means of a complicated limiting process on a small disk of vanishing radius. Shigehara defined his by means of a "bare coupling constant" whose physical meaning was not clear. One may, however, define a physical scattering operator without reference to any microphysics by defining it as the ratio of the strength of the incident field at the scatterer to the strength of the outgoing field in the vicinity of the scatterer. This is the standard definition for the scatterer's t matrix in an unbounded medium. The scatterer's cross section is closely related to its t matrix. This strategy has been used previously to formulate general time-dependent wave equations in terms of scattering matrices in the time domain [20]. Here we shall restrict the discussion to the simpler and more familiar case of a scattering matrix in the frequency domain. The advantage of such a formulation is that its physical meaning is unambiguous and natural and the formalism is straightforward and well known. We therefore consider the case of an infinite domain with an isotropic point scatterer at position \mathbf{b} . The field in the vicinity of the scatterer is then given by, in the absence of sources near the scatterer, the sum of an incident field and a scattered field

$$\psi = \psi^{\text{incident}} + \psi^{\text{scattered}}. \quad (5)$$

The incident field is regular at \mathbf{b} and is thus, to leading order in the distance from the scatterer,

$$\psi^{\text{incident}}(\mathbf{r}) = \psi^{\text{incident}}(\mathbf{b}) J_0(\omega |\mathbf{r} - \mathbf{b}|). \quad (6)$$

The scattered field is outgoing, isotropic, and a linear function of the incident field evaluated at the position of the scatterer. It is thus of the form

$$\psi^{\text{scattered}}(\mathbf{r}) = (-i/4)H_0^{(1)}(|\mathbf{r} - \mathbf{b}| \omega) t(\omega) \times \psi^{\text{incident}}(\mathbf{b}), \quad (7)$$

where the complex number $t(\omega)$ represents the scalar transition strength of the isotropic point scatterer. More complicated scatterers are often represented by a T matrix that gives the coefficients of a multipole outgoing field in terms of the coefficients of a multipole incident field [21].

The incident field may be decomposed in terms of incoming and outgoing waves

$$\begin{aligned} \psi^{\text{incident}}(\mathbf{r}) &= \psi^{\text{incident}}(\mathbf{b}) J_0(\omega |\mathbf{r} - \mathbf{b}|) \\ &= \psi^{\text{incident}}(\mathbf{b}) \\ &\quad \times \frac{1}{2} [H_0^{(2)}(\omega |\mathbf{r} - \mathbf{b}|) + H_0^{(1)}(\omega |\mathbf{r} - \mathbf{b}|)]. \end{aligned} \quad (8)$$

Substituting (8) and (7) into (5), one finds that the total field is representable as a sum of incoming and outgoing waves

$$\psi = \psi^{\text{incident}}(\mathbf{b}) \left[\frac{1}{2} H_0^{(2)}(\omega |\mathbf{r} - \mathbf{b}|) + \left\{ \frac{1}{2} - it/4 \right\} H_0^{(1)}(\omega |\mathbf{r} - \mathbf{b}|) \right], \quad (9)$$

the ratio of whose coefficients is the "scattering" or "s" matrix. Energy conservation requires that incoming and outgoing powers be equal

$$|\frac{1}{2}|^2 = |\frac{1}{2} - it/4|^2. \quad (10)$$

This implies an optical theorem

$$|t|^2 = -4 \text{Im} t \quad (11)$$

or

$$t = (\alpha + i/4)^{-1} \quad (12)$$

for some real α .

The cross section of the point scatterer is defined in the usual way as the ratio of outgoing power to incident flux. It is given in terms of the transition strength t by

$$\sigma = |t|^2 / 4\omega. \quad (13)$$

The maximum possible cross section of an isotropic point scatterer is therefore obtained at $\alpha = 0$, where $\sigma = 4/\omega = 2\lambda/\pi$.

If the same scatterer is placed in a finite system and an isotropic point source is placed at position $\mathbf{s} \neq \mathbf{b}$, the resulting field $G(\mathbf{r}, \mathbf{s})$ will have apparent sources at points \mathbf{b} and \mathbf{s} only

$$G(\mathbf{r}, \mathbf{s}) = G_0(\mathbf{r}, \mathbf{s}) + G_0(\mathbf{r}, \mathbf{b}) A(\mathbf{b}, \mathbf{s}), \quad (14)$$

where A is as yet an undetermined quantity. The first term of (14) is regular for \mathbf{r} near \mathbf{b} . Because it is a solution of the wave equation it is therefore, in the vicinity of \mathbf{b} , equal to a constant times the Bessel function J_0 . Adding and subtracting a Hankel function, Eq. (14) then becomes, for points \mathbf{r} near \mathbf{b} ,

$$\begin{aligned} G(\mathbf{r}, \mathbf{s})|_{\mathbf{r}=\mathbf{b}} &= G_0(\mathbf{b}, \mathbf{s}) J_0(\omega |\mathbf{r} - \mathbf{b}|) \\ &\quad - (i/4) H_0^{(1)}(\omega |\mathbf{r} - \mathbf{b}|) A(\mathbf{b}, \mathbf{s}) \\ &\quad + \{ G_0(\mathbf{r}, \mathbf{b}) + (i/4) H_0^{(1)}(\omega |\mathbf{r} - \mathbf{b}|) \} \\ &\quad \times A(\mathbf{b}, \mathbf{s}). \end{aligned} \quad (15)$$

Inasmuch as the response G_0 consists of a *direct* part [Eq. (4)] and a *reverberant* part consisting of all wall reflections, it may be recognized that the expression in curly brackets is the reverberant part only and is (as long as ω is not a natural frequency of the bare system in which case G_0 is undefined everywhere) regular at $\mathbf{r} = \mathbf{b}$. As it is also a solution of the wave equation, it is, for $\mathbf{r} \approx \mathbf{b}$, equal to a constant times $J_0(\omega |\mathbf{r} - \mathbf{b}|)$. We define

that purely reverberant part of G_0 as f :

$$f(\mathbf{b}) = \lim_{\mathbf{r} \rightarrow \mathbf{b}} \{ G_0(\mathbf{r}, \mathbf{b}) + (i/4)H_0^{(1)}(\omega|\mathbf{r}-\mathbf{b}|) \}, \quad (16)$$

which leads to a description of the field in the vicinity of the scatterer as the sum of an incident and a scattered part (recall that $J_0 = 1$ at $\mathbf{r} = \mathbf{b}$)

$$G(\mathbf{r}, \mathbf{s})|_{\mathbf{r} \approx \mathbf{b}} \approx [G_0(\mathbf{b}, \mathbf{s}) + f(\mathbf{b})A(\mathbf{b}, \mathbf{s})]J_0(\omega|\mathbf{r}-\mathbf{b}|) \\ + (-i/4)H_0^{(1)}(\omega|\mathbf{r}-\mathbf{b}|)A(\mathbf{b}, \mathbf{s}). \quad (17)$$

The ratio of the coefficients of these parts is, by definition, the scatterer strength t . So

$$t = A(\mathbf{b}, \mathbf{s})/[G_0(\mathbf{b}, \mathbf{s}) + f(\mathbf{b})A(\mathbf{b}, \mathbf{s})]. \quad (18)$$

But t is independent of the scatterer and source positions

$$tf(\mathbf{b}) = 1,$$

$$\alpha + i/4 = f(\mathbf{b}) = \lim_{\mathbf{r} \rightarrow \mathbf{b}} \{ G_0(\mathbf{r}, \mathbf{b}) + (i/4)H_0^{(1)}(\omega|\mathbf{r}-\mathbf{b}|) \} \\ = i/4 + \lim_{\mathbf{r} \rightarrow \mathbf{b}} \{ G_0(\mathbf{r}, \mathbf{b}) - (1/2\pi)[\gamma + \ln(|\mathbf{r}-\mathbf{b}|/\omega/2)] \}, \quad (22)$$

or

$$\alpha = g(\mathbf{b}, \omega) \\ = \lim_{\mathbf{r} \rightarrow \mathbf{b}} \{ G_0(\mathbf{r}, \mathbf{b}) - (1/2\pi)[\gamma + \ln(|\mathbf{r}-\mathbf{b}|/\omega/2)] \}, \quad (23)$$

where (23) defines the function $g(\mathbf{b})$ and γ is Euler's constant $\gamma = 0.5772157 \dots$. Equation (23) is presumably equivalent to Seba's [12] Eq. (8) and to Shigehara's [15] Eq. (14). This formulation, however, has the virtue of being a description in terms of a scattering parameter α directly related to scattering cross section and lacking any divergent modal sums. The relationship between these three formulations is discussed further below, following Eq. (30).

IV. EVALUATION OF THE CHARACTERISTIC EQUATION

G_0 is given by its modal decomposition, Eq. (3). The characteristic equation (23), however, is not readily evaluated by means of the direct modal decomposition

$$G_0(\mathbf{r}, \mathbf{b}) = \sum_{n,m} \phi_{nm}(\mathbf{r})\phi_{nm}(\mathbf{b})/[(\omega + i\epsilon)^2 - \omega_{nm}^2] \quad (24)$$

because that sum is slowly convergent and indeed divergent at $\mathbf{r} = \mathbf{b}$. The explicit logarithm in (23) cancels that divergence, so in the indicated limit the expression is regular. Nevertheless, numerical evaluation of the limit could be awkward. In order to accelerate the conver-

gence it is useful to consider a related problem, defined on the same rectangular domain without scatterer used to define G_0 . We consider the problem

$(-\nabla^2 + \Lambda^2)\Psi = \delta^2(\mathbf{r}-\mathbf{b})$, $\Psi = 0$ on boundary,

$$G(\mathbf{r}, \mathbf{s}) = G_0(\mathbf{r}, \mathbf{s}) + G_0(\mathbf{r}, \mathbf{b})\tau(\mathbf{b})G_0(\mathbf{b}, \mathbf{s}), \quad (19)$$

where the function $\tau(\mathbf{b})$ is the scattering operator as modified by the reflections from the walls

$$\tau(\mathbf{b}) = t/[1 - f(\mathbf{b})t]. \quad (20)$$

Resonance requires ω such that $tf(\mathbf{b}) = 1$. [One can show that such ω are not equal to any of the ω_{nm} of the bare rectangle unless $\phi_{nm}(\mathbf{b}) = 0$.] Thus the characteristic equation for the finite system with scatterer is

$(-\nabla^2 + \Lambda^2)\Psi = \delta^2(\mathbf{r}-\mathbf{b})$, $\Psi = 0$ on boundary,

$$\Psi = \sum_{n,m} \phi_{nm}(\mathbf{r})\phi_{nm}(\mathbf{b})/[\Lambda^2 + \omega_{nm}^2]. \quad (26)$$

The solution may also be represented as a sum of a direct contribution, equal to the solution to (25) in an unbounded domain, and the contributions from image sources

$$\Psi = (1/2\pi)K_0(|\mathbf{r}-\mathbf{b}|\Lambda) \\ + (\text{image source contributions}). \quad (27)$$

As $\mathbf{r} \rightarrow \mathbf{b}$, this becomes

$$\Psi = (-1/2\pi)[\gamma + \ln(|\mathbf{r}-\mathbf{b}|\Lambda/2)] \\ + (\text{image source contributions}). \quad (28)$$

By equating the two expressions for $\Psi(\mathbf{r} \approx \mathbf{b})$ [(26) and (28)] one may derive an expression for $\gamma + \ln(|\mathbf{r}-\mathbf{b}|\Lambda/2)$ in terms of a modal sum (26) and an image source sum. This in turn may be used in (23) together with the modal sum representation (24) for G_0 . The result is

$$g(\mathbf{b}, \omega) = \lim_{\mathbf{r} \rightarrow \mathbf{b}} \left[\sum_{n,m} \phi_{nm}(\mathbf{r})\phi_{nm}(\mathbf{b})/[\Lambda^2 + \omega_{nm}^2] \right. \\ \left. + \sum_{n,m} \phi_{nm}(\mathbf{r})\phi_{nm}(\mathbf{b})/[\omega^2 - \omega_{nm}^2] - (1/2\pi)\ln(\omega/\Lambda) - (\text{image source contributions}) \right]. \quad (29)$$

If we choose $\Lambda = \omega$, combine the two modal sums in (29), and then take the limit, we find

$$g(\mathbf{b}, \omega) = 2\omega^2 \sum_{n,m} \phi_{nm}^2(\mathbf{b}) / [\omega^4 - \omega_{nm}^4] - \sum_{\text{IS}} \mathcal{S}_{\text{imgsgn}}(1/2\pi) K_0(|\mathbf{r}_{\text{IS}} - \mathbf{b}| \omega), \quad (30)$$

where the second sum is over all positions \mathbf{r}_{IS} of the image sources and $\mathcal{S}_{\text{imgsgn}}$ is the sign of the source. This modal summation now converges, as does the image source sum.

A comparison of the present equations (23) and (30) with Shigehara's [15] Eq. (14) allows one to contrast the present formulation in terms of a scatterer characterization parameter α [related to cross section by Eqs. (12) and (13)] and Shigehara's parameter v_B^{-1} . The result is

$$v_B^{-1} = \alpha + \sum_{\text{IS}} \mathcal{S}_{\text{imgsgn}}(1/2\pi) K_0(|\mathbf{r}_{\text{IS}} - \mathbf{b}| \omega) - \sum_{n,m} \phi_{nm}^2(\mathbf{b}) [1/(\omega^2 + \omega_{nm}^2) - \omega_{nm}^2 / (1 + \omega_{nm}^4)].$$

At high frequencies the image source sum may be neglected. It nevertheless appears that the difference between α and v_B^{-1} depends on scatterer position and, logarithmically, on ω itself. Thus v_B is related to cross section, but in a complicated way. Except for these differences it appears that the formulations are otherwise equivalent.

A similar contrast can presumably be drawn after a comparison of Seba's [12] Eq. (8) with the present Eqs. (23) and (30). This would allow one to identify the cross section of Seba's scatterer in terms of the parameter α used to characterize it there. This comparison, however,

$$\begin{aligned} g &= \sum_{n,m} \phi_{nm}^2(\mathbf{b}) 4\omega^6 / [\omega^8 - \omega_{nm}^8] - \frac{1}{4} + (1/2\pi) \sum_N \sum_M [K_0(R\omega) - 2k(R\omega)]_{R=\{2NL_x + 2b_x, 2ML_y\}} \\ &+ (1/2\pi) \sum_N \sum_M [K_0(R\omega) - 2k(R\omega)]_{R=\{2NL_x, 2ML_y + 2b_y\}} \\ &- (1/2\pi) \sum_N \sum_M [K_0(R\omega) - 2k(R\omega)]_{R=\{2NL_x + 2b_x, 2ML_y + 2b_y\}} \\ &- (1/2\pi) \sum_N \sum_{M'} [K_0(R\omega) - 2k(R\omega)]_{R=\{2NL_x, 2ML_y\}}, \end{aligned} \quad (35)$$

where the image source sum and its signs have now been made explicit and the sums over N and M run from $-\infty$ to $+\infty$. The prime on the last sum indicates that the term $N=M=0$ is to be excluded. It is this expression that will be used in the next section to evaluate the characteristic equation $g = \alpha$.

V. SCATTERER AT THE CENTER: NUMERICAL RESULTS

We consider the special case, extensively studied by Seba and co-workers [12,13] and Shigehara [15], in which the scatterer is placed exactly at the center of the rectangle: $b_x = L_x/2$, $b_y = L_y/2$. In this case all $\phi_{nm}^2(\mathbf{b})$ vanish unless n and m are both odd, corresponding to the even-

does not appear to be simple.

The modal series expression (30) for g converges somewhat slowly. It may be further accelerated by considering another problem

$$(\nabla^4 + \Lambda^4)\Psi = \delta^2(\mathbf{r} - \mathbf{b}), \quad (31)$$

with conditions on the boundary of the rectangular domain $\Psi = 0$ and $\partial_n^2 \Psi = 0$, where ∂_n is a normal derivative. This problem represents the static response, to a concentrated point force, of a simply supported Euler-Bernoulli plate on an elastic foundation. It has a solution that may be represented by a modal decomposition

$$\Psi = \sum_{n,m} \phi_{nm}(\mathbf{r}) \phi_{nm}(\mathbf{b}) / [\Lambda^4 + \omega_{nm}^4]. \quad (32)$$

It may also be represented in terms of the solution one would have in an infinite domain, by adding a correction in the form of a sum over image source contributions

$$\begin{aligned} \Psi &= (-4/8\pi\Lambda^2) k(\Lambda|\mathbf{r} - \mathbf{b}|) \\ &+ \sum_{\text{IS}} (-4/8\pi\Lambda^2) \mathcal{S}_{\text{imgsgn}} k(|\mathbf{r}_{\text{IS}} - \mathbf{b}| \Lambda), \end{aligned} \quad (33)$$

where k is the Kelvin function of the second kind. Therefore at $\mathbf{r} = \mathbf{b}$ and $\Lambda = \omega$, one finds [because $k(0) = -\pi/4$]

$$\begin{aligned} \sum_{n,m} \phi_{nm}^2(\mathbf{b}) 2\omega^2 / [\Lambda^4 + \omega_{nm}^4] \\ = \frac{1}{4} - (1/\pi) \sum_{\text{IS}} \mathcal{S}_{\text{imgsgn}} k(|\mathbf{r}_{\text{IS}} - \mathbf{b}| \omega). \end{aligned} \quad (34)$$

We add this to the previous expression for g to obtain

even parity class, for which case $\phi_{nm}^2(\mathbf{b}) = 4/L_x L_y$. Only the even-even parity modes of the bare rectangle are affected by the scatterer. All the other modes of the bare rectangle vanish at the position of the scatterer and are therefore unaffected. It is only the even-even modes that are studied in the remainder of this paper.

All poles in the sum (35) have residues with the same sign. A plot of $g(\omega)$ therefore will be a simple succession of simple poles. (We presume the generic case in which the sides of the rectangle are incommensurate and there are no degeneracies in the bare rectangle). Between each pole g runs monotonically from ∞ to $-\infty$. A typical plot of $g(\omega)$ is shown in Fig. 1. The contributions from the image sums are finite (and indeed are very small if ωL is large and the scatterer is not near an edge). They are

furthermore slowly varying in ω . Thus the roots $g = \alpha$ must interleave with the poles of g . This is readily seen in the plot. Seba used this observation to establish that the roots must exhibit level repulsion. The same feature, however, also establishes that the system cannot have much spectral rigidity; the long-range spectral correlations must be approximately identical to those of the bare rectangle, i.e., essentially Poissonian. The feature also allows for a simple procedure for exhaustive root search-

ing. One need merely find the single root that must exist between each pair of known successive resonances of the bare rectangle, given by Eq. (2).

In practice the sums over n and m cannot be taken to infinity; they must be truncated. This is done by dropping all terms with $\omega_{nm} > \Omega$, where Ω is taken to be significantly greater than the largest ω of interest. The remainder of the sum is approximated by an integral over all \mathbf{k} in the first quadrant of k space such that $|\mathbf{k}| > \Omega$,

$$g \approx \sum'_{n,m} [4/L_x L_y] 4\omega^6 / [\omega^8 - \omega_{nm}^8] = \frac{1}{4} + (\text{image source sum}) + 2\omega^6 / \pi \int_{|\mathbf{k}| > \Omega} d^2k / [\omega^8 - k^8] \quad (36)$$

$$\approx \sum'_{n,m} [4/L_x L_y] 4\omega^6 / [\omega^8 - \omega_{nm}^8] - \frac{1}{4} + (\text{image source sum}) - (1/3\pi)(\omega/\Omega)^6 + [\text{higher-order terms in } (\omega/\Omega)], \quad (37)$$

where the prime on the sum over n and m indicates that terms with $\omega_{nm} > \Omega$ are to be omitted.

The error incurred with these truncations and approximations is of the order of $(\omega/\Omega)^7$. If $\Omega \gg \omega$ then the error is negligible. The error is in any case a smooth, slowly varying function of ω . As such it could be absorbed into a frequency-dependent α . It is thus unimportant in evaluating eigenvalue statistics; it will only affect the secularities in the spectrum. These secularities are in any case removed before the statistics are evaluated. In practice we find that Ω is easily taken sufficiently great that the error is negligible.

The sum over image sources is also small and weakly varying. The nearest image sources are at a distance of the order of L . The $k(\omega L)$ terms give the larger contributions to g , of the order of $\exp(-L\omega/\sqrt{2})$. This is much less than unity if $L\omega$ is large, so the image source sum is also safely ignored, at least at high frequency.

We calculated all even-even roots of the characteristic equation that lay between $\omega_{\min} = 60$ and $\omega_{\max} = 100$ in ten different rectangles, with sizes $L_x = \pi$, $L_y = \pi(1.01)^p / [(\sqrt{5} - 1)]$, where p was an integer between -4 and 5 . The parameter α was chosen to be zero. The parameter Ω was taken to be 140 after studies showed that larger values of Ω changed most of the higher calculated frequencies by much less than 1% of a mean level spacing. A small number (about 2% of the levels) were changed by as much as 2% of a mean level spacing. The lower frequencies were changed even less. The sum over image sources is even less important, the effect being to change the calculated resonance frequencies by much much less than 1% of a mean level spacing. From 1067 to 979 roots were found in each rectangle, depending on size. Each rectangle was separately desecularized, procedures being described elsewhere [4,16]. The staircase functions were fit to a quadratic function of frequency by expanding in a series of three Legendre polynomials. The inclusion of cubic and quartic terms had a negligible effect on the mean square residual. Level spacing histograms and number variances were constructed for each rectangle and combined. Because of the large number (10213) of levels found, it was possible to calcu-

late accurate values for conditional level density also. All these statistics are presented below.

Figure 2 shows the histogram of nearest-neighbor level spacings. It conforms closely to the Wigner distribution and so confirms Seba's conclusion that the system has some GOE character. We note, however, significant deviations from the Wigner distribution, especially at the larger ranges. In the range from 3 to 3.1, for example, 24 level spacings were observed, while the Wigner distribution predicts that only 3.3 will occur in a sample of 10203 spacings. The error in the observation is presumably one part in $\sqrt{24}$. This error is much less than the observed difference between observation and the Wigner distribution. Neighboring bins have similar character. One concludes that the Wigner distribution (and thus the GOE) does not correctly describe the level spacing distri-

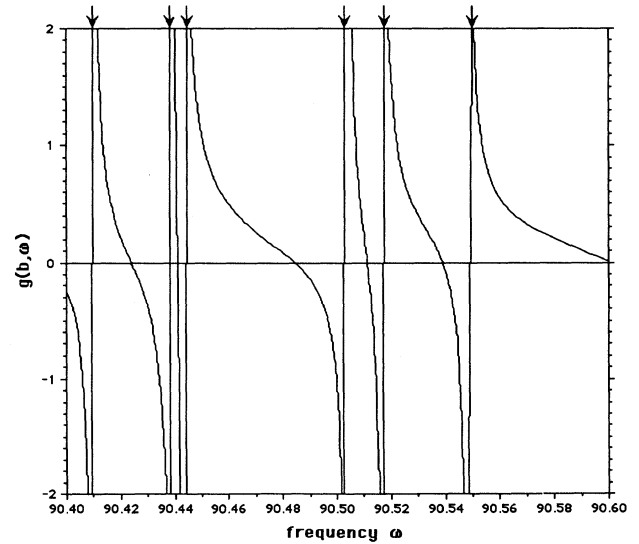


FIG. 1. A short range of the function $g(\mathbf{b}, \omega)$ is shown for the case $L_x = \pi$, $L_y = \pi/(\sqrt{5} - 1)$ with \mathbf{b} chosen at the center of the rectangle. Arrows indicate the positions of the poles of g , the resonances of the bare rectangle. The roots of the dressed rectangle occur at the places where $g = \alpha$.

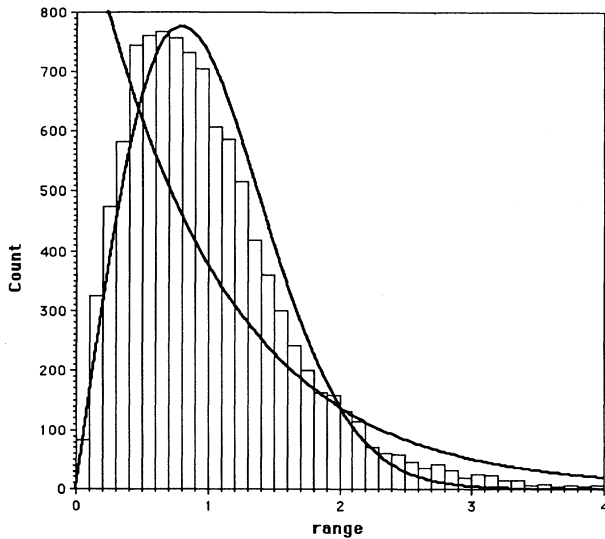


FIG. 2. Level spacing histogram for a total of 10213 even-even modes of ten rectangles, each with an isotropic point scatterer at its center. The Wigner distribution and the Poisson distribution are plotted for comparison.

bution. Seba's [12] Fig. 1 shows similar deviations between the Wigner distribution and the observed level spacing histogram, though the deviation is not discussed there. The deviation appears more severe in Seba's work; this is perhaps attributable to a smaller cross section in the scatterer used there.

Long-range correlations are better studied by means of the number variance. In Fig. 3 we plot the number variance observed among the 10213 levels observed in the rectangles with scatterers, as well as the number variance for the 10223 levels observed in the same frequency range in the undressed rectangles. The number variance

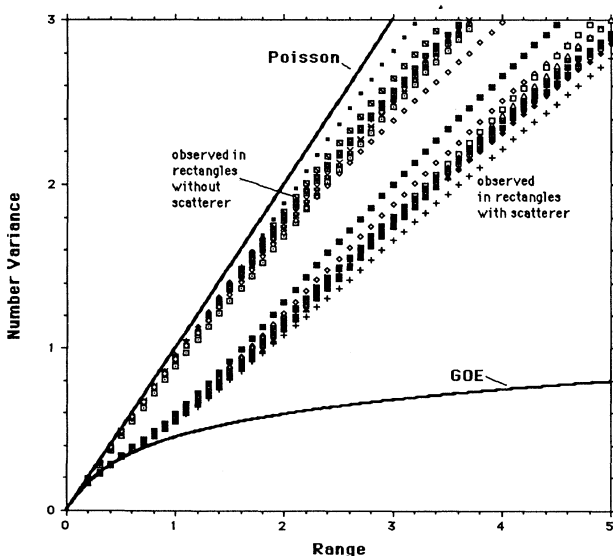


FIG. 3. Number variance for the dressed and undressed rectangles (20 systems in all, each with about 1000 levels) is compared to the GOE and Poisson predictions.

predicted by the GOE and by a Poisson process is also plotted [22]. Again we see that the rectangle with scatterer has eigenstatistics that correspond to the GOE over the shorter ranges but not the longer ranges. As anticipated, the number variance at longer ranges has much of the character of the Poisson process. The decided kink in the number variance at a range of about 0.7 is especially intriguing. It is as if the system with the point scatterer is trying to be GOE at shorter ranges and then has a sudden change of heart. This is consistent with the hypothesis advanced in Sec. II. Shigehara [15] shows similar behavior in plots of the Δ_3 statistic in his systems; a comparison of the observed correlation ranges with the cross sections of Shigehara's scatterers might be of interest.

The number variance Σ^2 may be expressed in terms of the conditional number density by means of a convolution. Σ^2 at range r is therefore perhaps not the best measure of spectral correlations at range r . A better quantity for evaluating the exact degree of spectral correlations over a spectral range r may be the conditional number density, given for the GOE by

$$\rho(\omega, \omega') = \rho [1 - Y_2(\rho\{\omega - \omega'\})], \quad (38)$$

where Y_2 is Dyson's two-level cluster function [3] and the mean level density ρ is unity in normalized units. By evaluating the conditional density of levels in the desecularized spectra one may construct an observed $\rho(\omega, \omega')$ and compare it with the above expression. One may furthermore construct standard error estimates for the calculated observed $\rho(\omega, \omega')$. These are given in Fig. 4.

The observed conditional level density is very nearly unity for all ranges in the undressed rectangles. In the dressed systems, however, it shows significant short-range order. Over ranges less than or equal to $r = \frac{1}{2}$ the observed conditional level density nearly agrees with the GOE prediction. Over very long ranges it goes to unity as it must. At intermediate ranges it shows a most remarkable deviation from GOE by overshooting the value unity. We do not venture an explanation for this overshoot, but do emphasize that, as predicted by the hypothesis in Sec. II, the GOE character of the conditional level density fails for longer ranges.

VI. CONCLUSIONS

It has been argued that GOE-like spectral correlations in a billiard will extend over a spectral range corresponding to the inverse of the time that a ray requires to explore all of phase space. For this reason systems with ray chaos, which rapidly explore phase space, have well developed GOE statistics. By the same token, pseudointegrable systems for which the rays may ergodically fill phase space, albeit perhaps not very rapidly, will show spectral correlations over shorter ranges. This, it is asserted, is the reason certain pseudointegrable systems studied in recent years have had GOE statistics.

Towards a confirmation of the hypothesis and in order to avoid issues of frequency scale (i.e., the ratio of wavelength to scatterer size), a system consisting of a rectangle with a single isotropic point scatterer at its center was in-

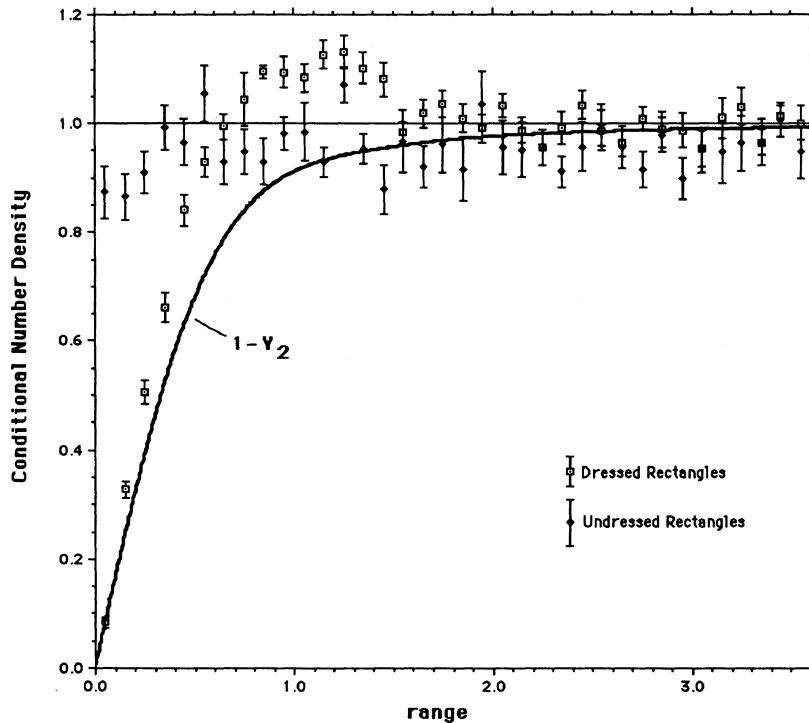


FIG. 4. Conditional number densities as observed among the ten dressed and ten undressed rectangles. The prediction of the GOE (solid bold line) is shown for comparison.

investigated. In accordance with the hypothesis, it was found that the system shows GOE spectra correlations out to a range of the order of unity.

The hypothesis has further implications that have not yet been explored. The prediction states that the non-dimensional range over which GOE statistics should apply is of the order of, and proportional to, the ratio of the diffuse scattering cross section to the wavelength. This number is $2/\pi$ for the system studied here. The prediction is thus essentially corroborated for only one value of this parameter. One cannot increase the scattering cross section of a single isotropic point scatterer beyond that

chosen here, but one could consider a system consisting of a number of such scatterers. It is predicted that the GOE character of the eigenstatistics of such a system should be maintained out to a range of the order of the number of scatterers in the system. An investigation of this prediction is planned to be the subject of a future paper.

ACKNOWLEDGMENT

This work has been supported by the National Science Foundation, Grant No. MSS 9114360.

-
- [1] *Chaotic Behavior in Quantum Systems: Theory and Application*, Vol. 120 of NATO Advanced Research Workshop on Quantum Chaos, edited by G. Casati (Plenum, New York, 1985).
- [2] M. C. Gutzwiller, *Chaos in Classical and Quantum Systems* (Springer-Verlag, Berlin, 1990).
- [3] *Chaos and Quantum Physics*, edited by M. G. Giannoni, A. Voros, and J. Zinn-Justin (Elsevier, Amsterdam, 1990).
- [4] T. A. Brody, J. Flores, J. B. French, P. A. Mello, A. Pandey, and S. S. M. Wong, *Rev. Mod. Phys.* **53**, 385 (1981).
- [5] M. L. Mehta, *Random Matrices* (Academic, Boston, 1990).
- [6] E. J. Heller, in *Quantum Chaos and Statistical Nuclear Physics*, edited by T. H. Seligman and H. Nishioka, *Lecture Notes in Physics* Vol. 263 (Springer, New York, 1986).
- [7] S. W. McDonald and A. N. Kaufmann, *Phys. Rev. Lett.* **42**, 1189 (1979); *Phys. Rev. A* **37**, 3067 (1988).
- [8] O. Bohigas, M. J. Giannoni, and C. Schmitt, *Phys. Rev. Lett.* **52**, 1 (1984).
- [9] H. J. Stockman and J. Stein, *Phys. Rev. Lett.* **64**, 2215 (1990); O. Legrand, C. Schmitt, and D. Sornette, *Europhys. Lett.* **18**, 101 (1992); A. Kudrolli, S. Sridar, A. Pandey, and R. Ramaswamy, *Phys. Rev. E* **49**, R11 (1994).
- [10] O. Bohigas, O. Legrand, C. Schmitt, and D. Sornette, *J. Acoust. Soc. Am.* **89**, 1456 (1991).
- [11] O. Bohigas, M. J. Giannoni, and C. Schmitt, in *Quantum Chaos and Statistical Nuclear Physics* (Ref. [6]).
- [12] P. Seba, *Phys. Rev. Lett.* **64**, 1855 (1990).
- [13] S. Albeverio and P. Seba, *J. Stat. Phys.* **64**, 369 (1991).
- [14] T. Cheon and T. D. Cohen, *Phys. Rev. Lett.* **62**, 2769 (1989).
- [15] T. Shigehara, *Phys. Rev. E* **50**, 4357 (1994).
- [16] R. L. Weaver, *J. Acoust. Soc. Am.* **85**, 1005 (1989).
- [17] E. J. Heller, in *Chaos and Quantum Physics* (Ref. [3]).
- [18] A. Shudo and Y. Shimizu, *Phys. Rev. E* **47**, 54 (1993).
- [19] The difficulty is related to the short distance logarithmic divergence of the Green's function in these geometries; $G(\mathbf{r}=\mathbf{r}')=\infty$. An attempt to find the scattering operator

$t\delta^2(\mathbf{x})$ associated with a delta-function potential $v\delta^2(\mathbf{x})$ leads to an equation for the scattering strength of the form $t = v + vG(\mathbf{r}=\mathbf{r}')t$, which has no solution. (In one dimension, however, where G does not diverge, the Kronig-Penny model δ -function scattering potential is definable. Shigehara manages the divergence by truncating his modal sum—in effect introducing an ultraviolet cutoff at the expense of losing physical meaning for the strength of his scattering potential; the strength v of his scatterer had to change with the assumed cutoff.) The effect is subtle and not widely appreciated. It may be further understood perhaps by considering the mathematical problem of the effect of a concentrated point force on the shape of a uniformly tensioned membrane. Laplace's equation for the shape indicates that the point force causes a funnel-shaped distortion that is logarithmically infinite at the point of application of the force. Thus a finite force causes an infinite

local displacement. Conversely, a finite local displacement requires only an infinitesimal force. The force necessary to hold a point fixed on a vibrating membrane is therefore zero. Fixing such a point therefore cannot change the eigenfrequencies of the membrane. It changes the eigenfunctions only by superposing an infinitesimal funnel-shaped distortion in the vicinity of the fixed point.

- [20] C. Vanneste, P. Sebbah, and D. Sornette, *Europhys. Lett.* **17**, 715 (1992); **18**, 567(E) (1992); D. Sornette, O. Legrand, F. Mortessagne, P. Sebbah, and C. Vanneste, *Phys. Lett. A* **178**, 292 (1993).
- [21] P. C. Waterman, *J. Acoust. Soc. Am.* **45**, 1417 (1969).
- [22] That the undressed system eigenstatistics are not precisely Poissonian has been discussed by G. Casati, B. V. Chirikov, and I. Guarneri, *Phys. Rev. Lett.* **54**, 1350 (1985). The deviation is expected to disappear at high frequency.